Middle East Journal of Science

https://dergipark.org.tr/mejs **MEJS**

e-ISSN:2618-6136

Research Article

MODELLING OF THE SOLAR CELL BASED ON CU_2SNS_3 THIN FILM PRODUCED BY SPRAY PYROLYSIS

***Serap YIGIT GEZGIN*[1] *Ilhan CANDAN*[2] *Silan BATURAY*[2] *Hamdi Sukur KILIC*[1,3,4,*]**

[1] Department of Physics, Faculty of Science, University of Selcuk, 42031 Selcuklu, Konya, Turkey
[2]Department of Physics, Faculty of Science, Dicle University, Diyarbakir, Turkey
[3]Directorate of High Technology Research and Application Center, University of Selcuk, 42031 Selcuklu, Konya, Turkey
[4]Directorate of Laser-Induced Proton Therapy Application and Research Center, University of Selçuk, 42031 Selcuklu, Konya, Turkey
*Corresponding author e-mail: hamdisukurkilic@selcuk.edu.tr

Abstract: *Cu_2SnS_3 (CTS) thin film has been produced for 30 sccm sulphur flux rate at 30 minutes annealing durations at 550 ^oC temperature. CTS thin film's crystalline structure has been investigated and crystalline size, lattice parameters, dislocation density and microstrain, crystalline number have also been determined. The CTS thin film's morphological and optical properties have been examined and thoroughly interpreted. Mo/CTS/CdS/AZO/Al solar cell has been modeled based on CTS thin film produced at the present work, using SCAPS-1D simulation program. V_{oc}, J_{sc}, FF, conversion efficiency, and photovoltaic parameters have been determined depending on neutral defect density at the interface, coefficient of radiative recombination, Auger electron/hole capture's coefficient, and operation temperature of CTS solar cell. As a consequence of the simulation study, the ideal efficiency of CTS solar cell has been determined to be 3.72 % and all the data obtained in this study have been presented, interpreted, and concluded to be original results.*

Keywords*: CTS, solar cell, SCAPS-1D, simulation*

Received: April 18, 2022 *Accepted: June 16, 2022*

1. Introduction

The photovoltaic (PV) market is based on solar cells manufactured with Silicon (Si), Copper Indium Gallium Selenium (CIGS), and Cadmium Tellur (CdTe) materials. Some prominent disadvantages of these mentioned elements are the high cost of In, Ga, and Te and the high processing cost of Si as well as the toxicity of the Cd element. Some materials such as Cu_2ZnSnS_4 (CZTS) have attracted great attention, which has properties such as low cost, easy to process, and being environmentally friendly. However, in recent years, since CZTS consists of many elements and its second phases are easily formed, research studies have been carried out on Cu_2SnS_3 (CTS) material for use in PV field. CTS is a p-type semiconductor with band gap values ranging from 0.9 to 1.7 eV and a high absorption coefficient ($>10^4$ cm^{-1}) [1]. Due to different arrangements of atoms in a lattice structure of CTS, different phases such as $Cu_4Sn_7S_{16}$, Cu_4SnS_4, Cu_3SnS_4 structure can also occur [2]. These phases can be considered a candidate for use as an absorber layer in solar cells.

The theoretically calculated efficiency of CTS solar cells is determined at about 30%. The reported highest power conversion efficiencies of CTS solar cell belongs to 6% Ge-doped CTS [3] and 5.24% Na-doped CTS [4] solar cells. Defects, voids, and second phases in CTS thin film cause some

limitations on efficiency. In order to overcome this problem, some parameters of technical and experimental apparatuses used in the thin film production are of great importance. Many techniques are described to achieve Cu_2SnS_3 thin films, for instance, reactive radio frequency magnetron sputtering [5], co-evaporation [6], wet chemical process [7], and spray pyrolysis [8]. Nonetheless, merely a limited number of studies have been reported on sprayed Cu_2SnS_3 materials [9]. In comparison to other methods, the Spin coating technique has numerous benefits including low production cost, easy deposition over large-area, and relatively simpler composition adjustment. Therefore, it is particularly more suitable for thin-film fabrication [10].

In recent years, simulation software used to calculate the efficiency of solar cells with the usage of layers forming solar cells has great importance. One of the most commonly used software in this field is SCAPS-1D (one-dimensional simulation software) only which among others calculates PV parameters of solar cell using physical parameters such as energy band gap, dielectric permittivity, the electron affinity of layers constructing solar cell, thin film thickness, the work function of contacts, etc [11, 12]. SCAPS-1D was developed at Gent University in the Department of Electronics and Information Systems. Depending on parameters such as operation temperature, Auger electron/hole capture coefficient, and interfacial defect density [13], PV parameters of solar cells can be calculated, and thus, a reliable prediction can be made on the performance of the solar cell.

In this study, CTS thin films have been grown for 30 sccm sulphur flux rate at 30 minutes annealing durations at 550 ^oC temperature. The structural, optical, and crystalline properties of thin film have been determined and interpreted. It is important to determine how the experimentally produced thin film will affect the efficiency by modelling it in the solar cell structure using the characteristic parameters of thin film. At this point, Mo/CTS/CdS/AZO/Al structure has been formed with the most ideal CTS thin film determined by using SCAPS-1D simulation program to show the effect of this thin film on the efficiency of CTS thin film solar cell. PV parameters of CTS solar cells have been calculated and their curves have been plotted, depending on temperature, Auger electron/hole capture coefficient, and interfacial defect density. It has been determined that PV performance of CTS solar cells depends on defects, recombination mechanism, and operation temperature. Thus, based on these parameters which significantly affect the efficiency, it has reached the conclusion that it is possible to obtain consistent interpretations of behaviour of solar cells. As a result, since CTS is a new material in solar cell applications, such a study on CTS solar cells with SCAPS program is very rare in literature, and it can be predicted that this study shed light on the experimental efficiency improvement studies of solar cells.

2. Materials and Methods

2.1. Experimental

CTS thin films have been fabricated on a glass substrate using a solution comprising 0.389 g copper(II) acetate ($Cu(CH_3COO)2\cdot H_2O$), 0.220 g tin(II) chloride dehydrate ($SnCl_2.2H_2O$), and 0.444 g thiourea (CH_4N_2S) deposited under optimized conditions with different Sulphur flux rate and time. All chemicals are separately dissolved in a mixture of ethanol and glacial acetic acid for 6h at room temperature in magnetic stirring. Firstly, thiourea solution was slowly mixed into copper(II) acetate solution, then, tin(II) chloride dehydrate was poured into the thiourea/copper(II) acetate solution. Finally, obtained solutions were stirred at room temperature for 4h until a homogenous clear solution was obtained. To regulate pH values, a few drops of diethanolamine were added to the mixture solution for the final solution. The molar ratios of Cu/Sn/S elements in solutions were adjusted due to a ratio of 2/1/6. Thiourea has volatile nature at high temperatures [14]. Therefore, this component was added twice to avoid any possible loss of sulphur.

Before the deposition process, glass substrates were washed by boiling in sufficient quantities of a mixture of H_2O, NH_3, and H_2O_2 at 105 °C, and then, in sufficient quantities of a mixture of H_2O, H_2O_2, and HCl at 105 °C to eliminate any residual waste. Then, glass substrates were cleaned in deionized water for 3 min and later dried. After obtaining final solutions and cleaning of substrates, the obtained solution was deposited via spin coating at a rate of 1500 rpm for 63 s in air. Final solutions were deposited onto the glass substrate layer by layer, and each layer was preheated to 220 °C for 10 min. After this process, obtained films were annealed under 30 and 40 sccm (standard cubic centimeters per minute) in 10 % H_2S + 90 % Ar atmosphere at 550 °C temperature in the furnace. CTS thin films were annealed under 30 sccm 10 % H_2S + 90 % Ar atmosphere at 550 °C temperatures for 15, 30 and 60 min and 40 sccm 10 % H_2S + 90 % Ar atmosphere at 550 °C temperatures for 15, 30 and 60 min, respectively. The obtained sample has been labelled and is demonstrated in Table 1 with Sulphur flux rate and time.

Table 1. Fabrication parameters for CTS film.

Thin films	Sulphur annealing temperature and time	Sulphur flux rate
CTS	550 °C for 30 min	30 sccm H_2S: Ar

The effect of Sulfurization on the structural, morphological, optical, and photoluminescence properties of CTS thin film have been studied in this work. The crystalline properties of acquired CTS film have been studied by X-Ray Diffractometer (XRD) unit (Bruker D8 Advance) operated at 40 kV and 40 mA. XRD was set up with a range of θ-2θ in steps of 0.02° to analyse the structural and phase purity analysis of CTS thin film structure. In addition, obtained films were investigated by using Confocal Raman Microscope and the obtained results were analysed. The surface topology and EDX measurements of all obtained films were obtained by FEI Quanta 250 FEG Scanning Electron Microscopy (FEI Co., Eindhoven, Netherlands). Conclusions of transmittance, energy band gap, and Urbach energy of thin films were analysed by Shimadzu UV-3600 spectrophotometer (Shimadzu, Tokyo, Japan) between 300-1100 nm.

2.2. Numerical Modelling and Material Parameters

SCAPS-1D software calculates PV parameters (V_{oc}, I_{sc}, FF, and η) of solar cells using physical parameters such as dielectric permittivity, band gap, the electron affinity of semiconductor layers in solar cells, work function of contacts, etc [15]. This software, which is a package program, performs a calculation procedure based on the solution of the Poisson equation (Eq. (1)), hole and electron continuity equations (Eq. (2) and Eq. (3)) [16], respectively:

$$\frac{\partial}{\partial x}\left(\varepsilon_0 \varepsilon_r \frac{\partial \Psi}{\partial x}\right) = -q\left(p - n + N_D^+ - N_A^- + \frac{\rho_{def}}{q}\right) \quad (1)$$

$$-\frac{\partial J_p}{\partial x} - U_p + G = \frac{\partial p}{\partial x} \quad (2)$$

$$-\frac{\partial J_n}{\partial x} - U_n + G = \frac{\partial n}{\partial x} \quad (3)$$

where ε_r and ε_0 are permittivity of semiconductor and vacuum, respectively, Ψ is electrostatic potential, N_A^- and N_D^+ indicate densities of ionized impurities of acceptors and donors, n and p are carrier concentrations of electrons and holes, and ρ_{def} is charge density of defects, J_p and J_n indicate hole and electron current densities, respectively, and G is generation rate.

Calculation of PV parameters of optical devices such as p-n heterojunction solar cells, perovskite solar cells, and dye solar cells can be performed courtesy of SCAP-1D software.

3. Results and Discussion

3.1. XRD and Raman Analyses

CTS thin film has been formed in tetragonal Cu_2SnS_3 crystal structures as seen XRD pattern and Raman spectrum in Figures 1a and 1b. (112), (200), (220) and (312) crystalline orientates in CTS thin film have been formed on 2θ = 28.8 º, 33.3 º, 47.6 º, 56.4 º angles, respectively. The crystal sizes of CTS films have been calculated by the Scherer equation:

$$S = 0.94\lambda/\beta cos\theta \quad (4)$$

where $S, \lambda, \beta,$ and θ parameters are the size of crystalline, X-Ray wavelength, full-width at half-maximum (FWHM) of diffraction peak, and angle of Bragg diffraction, respectively. The main crystalline size of CTS was calculated to be 55.56 nm.

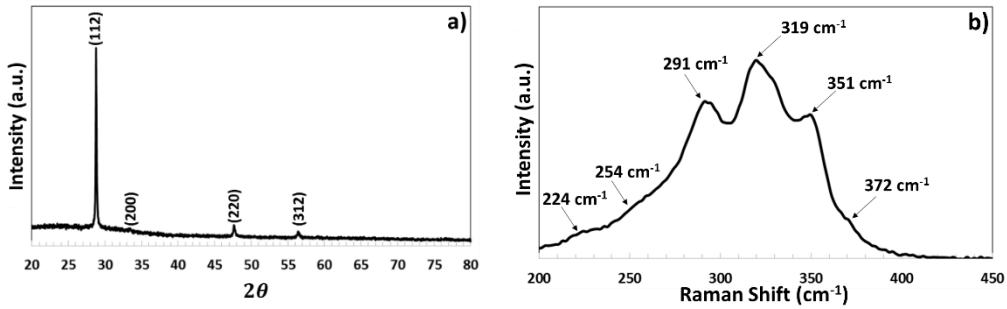

Figure 1. XRD pattern and Raman spectrum of CTS thin film

The micro-strain and dislocation density of CTS thin film [17, 18] were obtained by Eq. (5) and Eq. (6) as following:

$$\varepsilon = \frac{\beta cos\theta}{4} \quad (5)$$

$$\delta = \frac{1}{D^2} \quad (6)$$

The microstrain (ε) and dislocation density (δ), which express the formation of trap, vacancy, dangling bond, and defects in CTS thin film that negatory affect the development of the crystal structure. ε and δ values have been determined to be 0.65×10^{-3} and 3.24×10^{16} lines/m^2, respectively (as given in Table 2). The large crystal size leads to that there are few defects and traps in the grain boundary of thin film which ensures that ε and δ are low. Thus, minority charge carriers in CTS thin film have a longer lifetime and this leads to the higher efficiency of solar cells produced based on the absorber layer.

The crystal number per unit surface area (N) is calculated by Eq. (7),

$$N = \frac{T}{D^3} \quad (7)$$

where T is the thickness of CTS thin film. N value expresses the crystallization amount, which varies depending on the thickness and crystal size. The average thickness of CTS thin film has been measured to be ~1 μm. N values of thin film have been calculated as 0.58×10^{16} m^{-2} (Table 2). The large crystal size relative to film thickness which causes the crystalline number to be somewhat small.

Table 2. Crystalline size, dislocation density, micro-strain, and crystalline number of CTS thin film

Sample	Crystalline Size (nm)	*Dislocation density* $\times 10^{16}$ *(lines/m²)*	*Micro-strain* $\times 10^{-3}$	*Crystalline Number* $\times 10^{16}$ *(m⁻²)*
CTS	55.56	3.24	0.65	0.58

Raman spectrum in Figure 1b indicates that phase structures formed in CTS thin film in the 200-450 nm wavelength range. The monoclinic Cu_2SnS_3 (254 cm^{-1} [19], 291 cm^{-1}[2], 372 cm^{-1} [2]), tetragonal Cu_2SnS_3 (319 cm^{-1} and 351 cm^{-1}[2]) and SnS phase (224 cm^{-1}) formations have been occurred in CTS thin film. Due to dominant peaks on 319 cm^{-1} and 291cm^{-1}, it can be stated that CTS thin film is predominantly tetragonal phase structure which is compatible with the XRD pattern.

3.2. Photoluminescence Analyses

Photoluminescence (PL) is based on the principle that electrons are excited to upper energy levels by absorbing light incident on thin film, and then electron emits photons when it relaxes to a lower energy level. PL spectra of CTS thin film are presented in Figure 2. CTS thin film exhibits emission between 860 nm and 920 nm and PL has occurred at 1.40 eV (881 nm) under excitation. This energy is slightly above its band gap. Furthermore, PL formation of about 1.4 eV leading an increase in J_{sc} and power conversion efficiency in the solar cell.

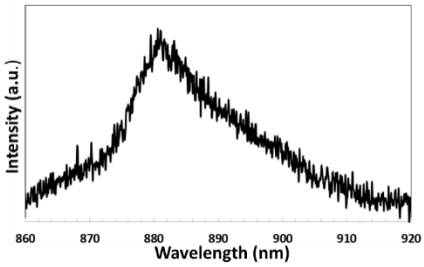

Figure 2. PL spectrum of CTS thin film

3.3. Morphologic and EDX Analyses

According to the SEM image in Figure 3a, CTS thin film consists of dense particles and particle size is a distribution between 300-500 nm indicating non-homogeneous particle size distribution.

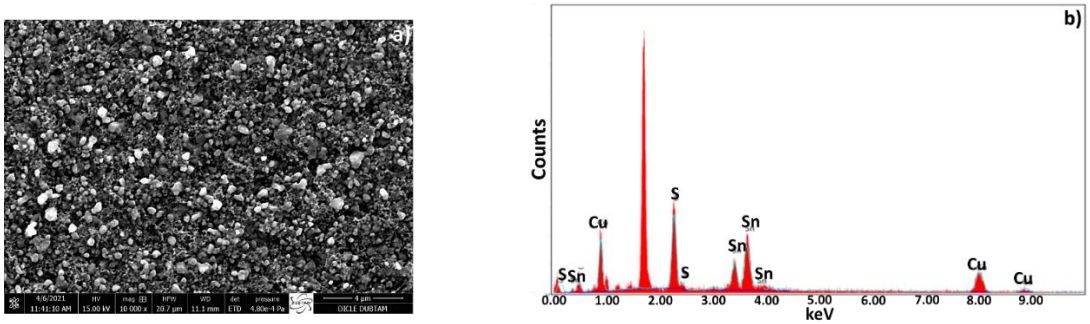

Figure 3. SEM image and EDX spectrum of CTS thin film

As seen in the EDX spectrum given in Figure 3b and Table 3, CTS thin film is Cu-poor and Sn-rich. Copper vacancies (V_{cu}), which act like acceptor defects, enhance the p-type conductivity of CTS thin film and improve the efficiency of the solar cell. However, when Sn atoms occupy V_{Cu} vacancies [20, 21], Sn_{Cu} donor defects form which can act as a recombination centre, and increase n-type

conductivity. In addition, the amount of elemental sulphur is high because the thin film is annealed under sulphur flux for a long time and at a high temperature.

Table 3. The atomic weight rates of elements in CTS thin film

Sample	*Cu(%)*	*Sn(%)*	*S(%)*	*Cu/Sn*	*S/metal*
CTS	25.65	15.25	59.10	1.68	1.44

3.4. Optical Analyses

The light absorbance of CTS thin film is decreased slightly towards to near-infrared region, as shown in Figure 4a. However, it showed a similar absorbance in visible and near-infrared regions. Tauc equation denoted by Eq. (8) that is used to obtain band gap of thin film:

$$\alpha h\nu = A\left(h\nu - E_g\right)^{1/2} \tag{8}$$

where $h\nu$ is photon energy, E_g is thin film energy band gap, A is a constant. E_g is obtained by a straight line of $(\alpha h\nu)^2$ versus $(h\nu)$ in Tauc plot in Figure 4b. CTS thin film's band gap has been determined to be 1.12 eV. This value proves that thin film absorbs a high number of photons in longer wavelength regions and is compatible with a band gap of Cu_2SnS_3 given in the literature [22].

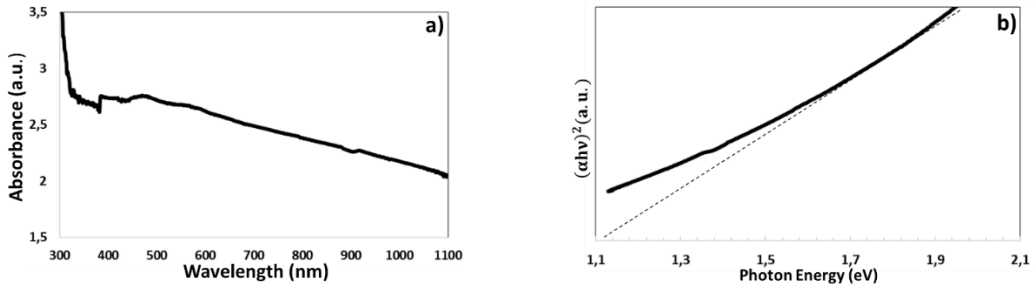

Figure 4. a) Absorption spectra and b) Tauc plot of CTS thin film

The thin film's absorption coefficient is determined by Eq. (9):

$$\alpha = 2.303(A/T) \tag{9}$$

T is the thickness of thin film and A is the absorbance of material. As expressed in the spectrum sketched in Fig. 5, CTS thin film has an absorption coefficient greater than 5.5×10^4 cm^{-1} in the visible region and this result is compatible with Cu_2SnS_3 absorption coefficients reported in the literature [1]. It has been observed that the absorption coefficient decreases towards to near-infrared region.

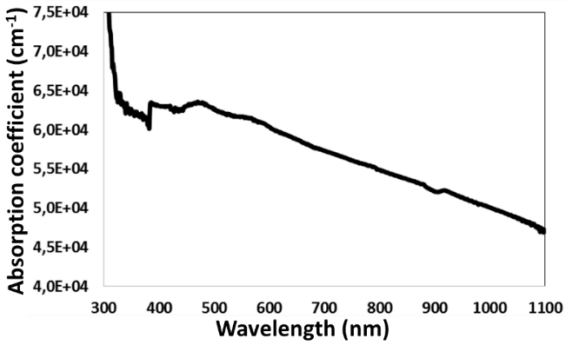

Figure 5. Absorption coefficient spectrum of CTS thin film

3.5. SCAPS-1D Simulation Program

3.5.1 Simulation of Mo/CTS/CdS/AZO/Al thin film solar cell

Absorber layers of solar cells, such as CTS, significantly affect power conversion efficiency. In many studies reported in the literature, only one layer of the solar cell was experimentally produced and the efficiency of the solar cell was determined by the physical parameters of that layer [15, 25, 26]. In this study, CTS thin film was determined to be the most ideal thin film depending on crystal structure and minimum defect conditions in CTS thin films.

Table 4. The physical parameters used in the modelling of Mo/CTS/CdS/AZO/Al solar cell

Layers	**AZO [23]**	**CdS [24]**	**CTS [23]**
Band Gap (eV)	3.3	2.4	1.12
Electron affinity (eV)	4.6	4.4	4.5
Dielectric permittivity (relative)	9	10	10
CB effective density of states (cm^{-3})	$2.20x10^{18}$	$1.80x10^{18}$	$2.20x10^{18}$
VB effective density of states (cm^{-3})	$1.80x10^{19}$	$2.40x10^{19}$	$1.80x10^{19}$
Electron/Hole thermal velocity (cm/s)	$1.00x10^{7}$	$1.00x10^{7}$	$1.00x10^{7}$
Electron/Hole mobility (cm^2/Vs)	100/25	100/25	100/25
Shallow donor density (cm^{-3})	$1.00x10^{20}$	$1.00x10^{18}$	0
Shallow acceptor density (cm^{-3})	0	0	$1.00x10^{16}$
Thickness	200 nm	50 nm	1 µm

Contacts	**Back Contact (Mo)**	**Front Contact (Al)**
Metal work function (eV)	5.00	4.08
Surface recombination velocity of electrons (cm/s)	$1x10^{7}$	$1x10^{5}$
Surface recombination velocity of holes (cm/s)	$1x10^{5}$	$1x10^{7}$

Therefore, we have formed Mo/CTS/CdS/AZO/Al solar cell structure based on CTS thin film absorber layer (in Figure 6), using SCAPS-1D program. The absorption coefficient spectrum file (shown in Figure 5) with 1 µm thickness and 1.12 eV band gap of CTS thin film was processed by SCAPS-1D simulation. Since Aluminium has a low work function, Al metal contact is preferred due to the possibility of exhibiting ohmic behaviour for the AZO semiconductor. We have calculated and interpreted PV performance depending on interface defect density, radiative recombination, Auger recombination, and operation temperature (parameters significantly change the efficiency) of Mo/CTS/CdS/AZO/Al the solar cell. Theoretically calculated results have been given below. Thus, by taking basic parameters of other layers for the simulated structures, the PV parameters of the solar cell are determined. This will provide a reliable and accurate path for the experimental operation of this type of solar cell. Physical parameters of layers forming CTS the solar cell in our model are given in Table 4.

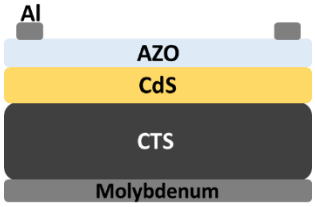

Figure 6. Mo/CTS/CdS/AZO/Al modelled by SCAPS-1D simulation

3.5.2 The effect of defect density (N_t) at the interface CTS/CdS of the solar cell

A high density of defect points can be localised at the interface between CTS and CdS layers leading to recombination centres [27]. Neutral defects can also occur at the interface of the second phase. The neutral defects acting as centres of Shockley-Read-Hall (SHR) recombination cause a certain decrease in the efficiency of the solar cell. These defects, located close to band edges, contribute to SHR recombination since the carrier is likely to return to its respective bands for shallow levels. Besides these, neutral defects can also be caused by lattice mismatch of CTS and CdS semiconductors in contact with each other [28, 29]. PV parameters of CTS solar cell versus interfacial neutral defect density (in 10^{10} and 10^{18} cm^{-3}) are given in Figure 7. According to these curves, V_{OC} and I_{SC} PV parameters of CTS the solar cell decreased after 1.10^{13} cm^{-3} of neutral defect densities.

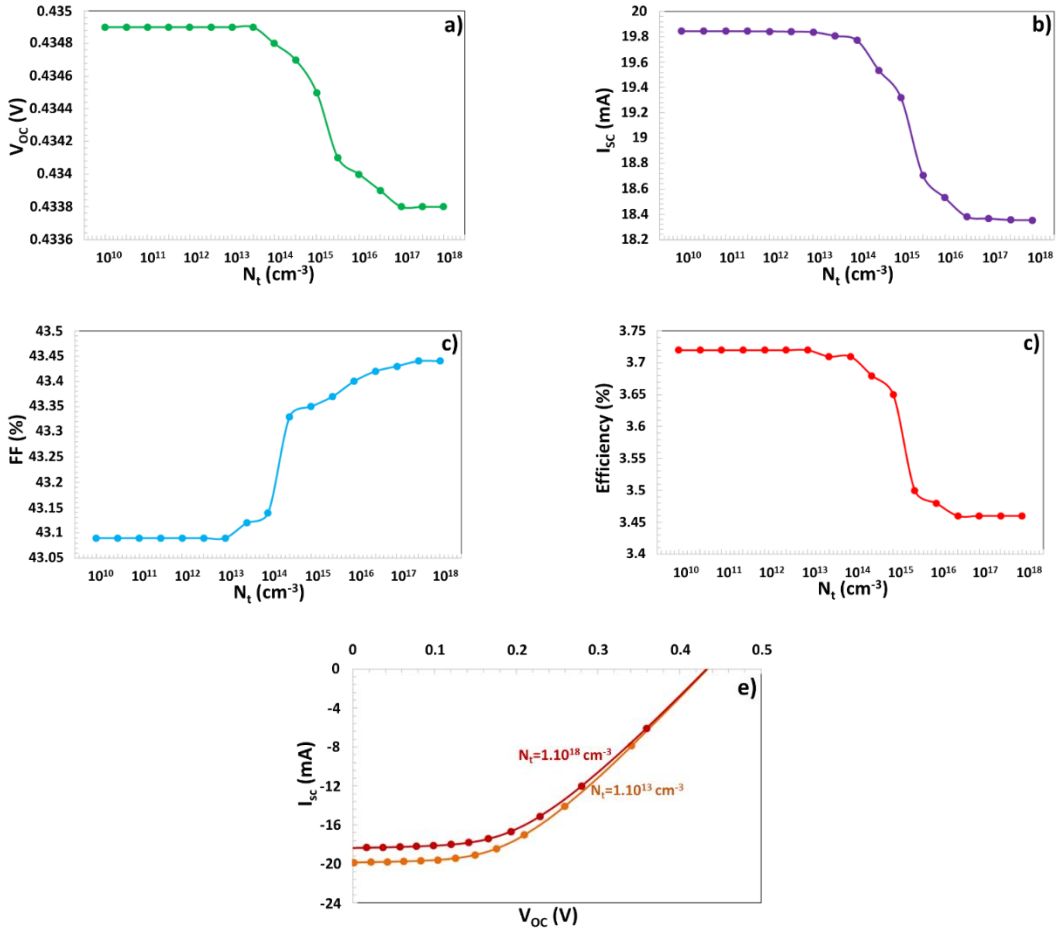

Figure 7. a) V_{oc}, b) I_{sc}, c) FF, d) Efficiency curves and e) I_{sc} depending on the interfacial defect density (N_t (cm^{-3}) at CTS/CdS of the solar cell.

Power conversion efficiency (shown in Figure 7e) of the solar cell for 1.10^{13} cm^{-3} defect density is 3.72 %. As seen in Figure 7d, after a neutral defect density of 1.10^{13} cm^{-3}, there was a sudden drop in the efficiency of the CTS solar cell. It has been noticed that the efficiency of the solar cell has remained constant at 3.46 % between 1.10^{17} and 1.10^{18} cm^{-3} of defect density [30]. As a result, neutral defect density should not be less than 1.10^{13} cm^{-3}. Therefore, it has been concluded that there is no reduction in power conversion efficiency.

3.5.3 Recombination mechanism for Mo/CTS-A2/CdS/AZO/Al solar cell

The recombination mechanism consists of three types of recombination radiative recombination, Auger recombination, and SRH recombination. These recombination mechanisms have a great influence on the PV performance of multilayer solar cells. In this study, the radiative recombination coefficient and Auger coefficient were evaluated. When an electron in the conduction band is transferred to the valence band, it emits a photon. The recombination of electrons and holes in this process is expressed as radiative recombination [31]. The efficiency spectra of the CTS solar cell depending on radiative recombination coefficient (Br (cm^3/s)) is given in Figure 8a and efficiency remains almost constant between 10^{-12} and 10^{-8} cm^3/s, it drops abruptly with 10^{-8} cm^3/s. For efficiency not to decrease, the Br value must be less than 10^{-8} cm^3/s. Auger recombination is a non-radiative event, which has a large effect on small band gap semiconductors.

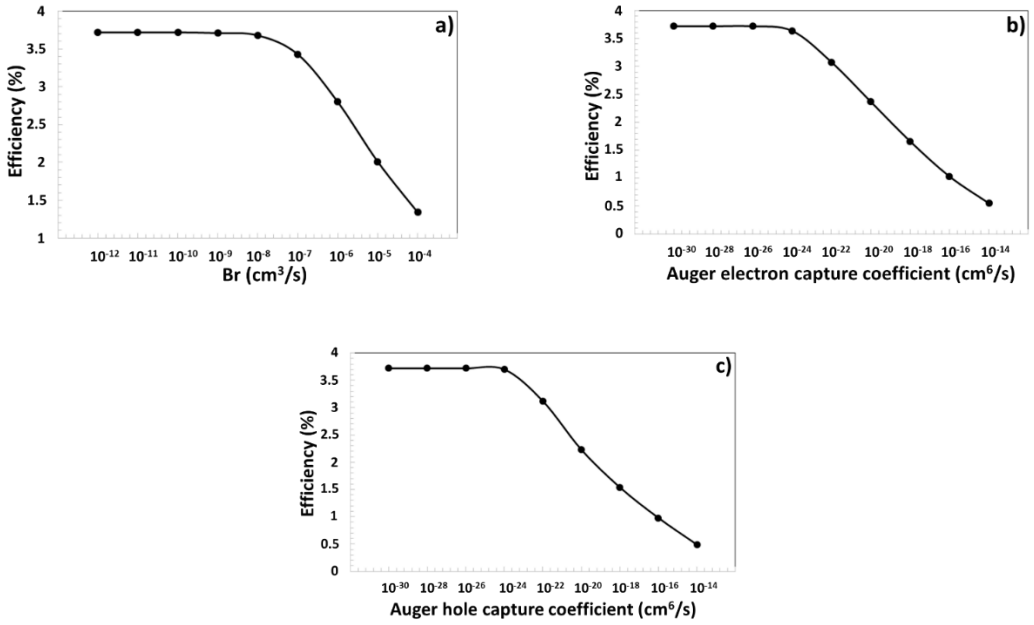

Figure 8. The efficiency curve of CTS solar cell depends on a) radiative recombination coefficient (Br), b) Auger electron and c) hole capture coefficient

When an electron and hole recombine with excess energy, an electron rises to the conduction band, or the hole transitions deeper into the valence band, but no light is produced [32, 33]. This process is known as Auger recombination. As seen in Figure 8b and 8c, when Auger electron and hole capture coefficients increase from 10^{-26} to 10^{-14} cm^6/s and 10^{-24} to 10^{-14} cm^6/s, respectively, efficiency values decrease. Therefore, these values should not be exceeded in order to avoid a significant decrease in the efficiency of the solar cell.

3.5.4 The effect of the operating temperature on CTS solar cell

Operation temperature adversely affects the performance of solar cells due to PV characteristics based on operation temperature between 240 °K and 400 °K in Figure 9, V_{OC} and FF values of CTS solar cell decreases as operation temperature increases. So, with increasing operation temperature, the band gap of the semiconductor decreases. In other words, the crystal lattice of the thin film broadens and the interatomic bonds are weakened. Weak bonds between atoms express that very low energy is required to break a bond and take an electron from the conduction band. Thus, the recombination rate of electron-hole pair between conduction and valence band increases. It limits access of minority charge carriers to

the depletion region. Moreover, an increase in dark current causes an increment in leakage current and reduces $the\ V_{OC}$ value [23, 34-36]. Furthermore, the energy of carriers increases even more and they become unstable as operation temperature increases. Therefore, carriers undergo recombination before they can reach the depletion region, this case reduces I_{sc} and V_{oc} values [36]. As a result, an increment in operation temperature deteriorates the performance of the solar cell. The efficiency of the solar cell was calculated to be 3.72 % for room temperature (300 K) [37-39].

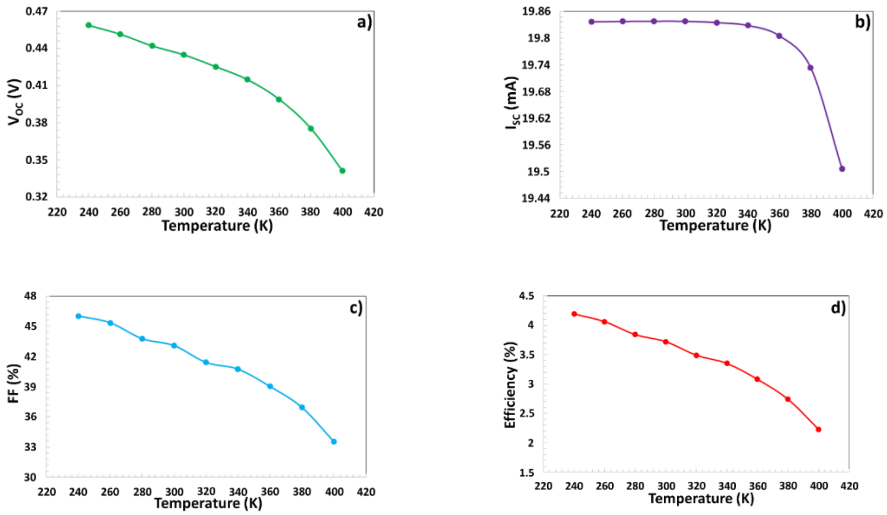

Figure 9. Effect of the operating temperature on a) V_{oc}, b) I_{sc}, c) FF, and d) efficiency parameters of CTS solar cell

4. Conclusion

CTS thin films were produced for 30 and 40 sccm sulphur flux rates in 15, 30, and 60 minutes annealing time durations at a constant 550 ºC temperature. CTS thin film has been formed in tetragonal in Cu_2SnS_3 crystalline structure. Crystalline size, dislocation density, microstrain, and the crystalline number of CTS structure have been calculated to be 55.56 nm, 3.24×10^{16} lines/m^2, 0.65×10^{-3}, and 0.58×10^{16} m^{-2}, respectively. CTS thin film consists of particles with dense and inhomogeneous size distribution. CTS thin film is Cu-poor and Sn rich, which has a band gap of 1.12 eV.

Mo/CTS/CdS/AZO/Al solar cell based on CTS layer was modelled using SCAPS-1D software. V_{OC} and I_{SC} PV parameters of CTS the solar cell were decreased with 10^{13} cm^{-3} of neutral defect density. Efficiency corresponding to this defect density is 3.72 %. Radiative recombination coefficient and Auger electron/hole capture recombination coefficient have been calculated: radiative recombination coefficient dropped abruptly beyond 10^{-8} cm^3/s value. For efficiency not to decrease, $the\ B_r$ value must be higher than 10^{-8} cm^3/s. When Auger electron and hole capture coefficients increase from 10^{-26} to 10^{-14} cm^6/s and 10^{-24} to 10^{-14} cm^6/s, respectively, efficiency values decrease. As the operation temperature increases, $the\ V_{OC}$ and FF of the solar cell decrease. CTS solar cell shows an efficiency value of 3.72 % at room temperature.

Acknowledgments

The authors wish to kindly thank; Dr. Marc Burgelman's group, the University of Gent, Belgium for providing the SCAPS-1D simulation program. Selcuk University Scientific Research Project (BAP) Coordination for the support with the number 15201070 and 19401140 projects, Selçuk University, High Technology Research and Application Centre (İL-TEK), and SULTAN Centre for infrastructure. Dicle

University Scientific Research Project (BAP) Coordination for the support with the number FEN.18.007 project,

Ethical Statements

The author declares that this document does not require an ethics committee approval or any special permission. Our study does not cause any harm to the environment.

Conflict of interest

The authors declare no conflict of interest.

Authors Contributions

SYG carried out calculations and wrote the first draft of the manuscript. IC and SB carried out the experiments. HSK supervised the projects. All authors discussed the results and contributed to the final manuscript.

References

[1] S. Rahaman, M. K. Singha, M. A. Sunil, and K. Ghosh, "Effect of copper concentration on CTS thin films for solar cell absorber layer and photocatalysis applications," *Superlattices and Microstructures*, 145, 106589, 2020.

[2] V. R. M. Reddy *et al.*, "Review on Cu2SnS3, Cu3SnS4, and Cu4SnS4 thin films and their photovoltaic performance," *Journal of Industrial and Engineering Chemistry*, 76, 39-74, 2019.

[3] M. Umehara, Y. Takeda, T. Motohiro, T. Sakai, H. Awano, and R. Maekawa, "Cu2Sn1-xGexS3 (x= 0.17) thin-film solar cells with high conversion efficiency of 6.0%," *Applied Physics Express*, 6(4), 045501, 2013.

[4] A. Kanai and M. Sugiyama, "Na induction effects for J–V properties of Cu2SnS3 (CTS) solar cells and fabrication of a CTS solar cell over-5.2% efficiency," *Solar Energy Materials and Solar Cells*, 231, 111315, 2021.

[5] J. Zhou, L. You, S. Li, and Y. Yang, "Preparation and characterization of Cu2ZnSnS4 microparticles via a facile solution route," *Materials Letters*, 81, 248-250, 2012.

[6] Z. Seboui, A. Gassoumi, and N. Kamoun-Turki, "Evolution of sprayed Cu2ZnSnS4," *Materials science in semiconductor processing*, 26, 360-366, 2014.

[7] K. Tanaka, Y. Fukui, N. Moritake, and H. Uchiki, "Chemical composition dependence of morphological and optical properties of Cu2ZnSnS4 thin films deposited by sol-gel sulfurization and Cu2ZnSnS4 thin film solar cell efficiency," *Solar Energy Materials and Solar Cells*, 95(3), 838-842, 2011.

[8] K. Woo, Y. Kim, and J. Moon, "A non-toxic, solution-processed, earth-abundant absorbing layer for thin-film solar cells," *Energy & Environmental Science*, 5(1), 5340-5345, 2012.

[9] Y. Wang and H. Gong, "Cu2ZnSnS4 synthesized through a green and economic process," *Journal of alloys and compounds*, 509(40), 9627-9630, 2011.

[10] S. Rabaoui, H. Dahman, N. Ben Mansour, and L. El Mir, "Structural, optical and electrical properties of Cu2SnS3 nanoparticles synthesized by simple solvothermal technique," *Journal of Materials Science: Materials in Electronics*, 26(2), 1119-1124, 2015.

[11] A. C. Piñón Reyes *et al.*, "Study of a lead-free perovskite solar cell using CZTS as HTL to achieve a 20% PCE by SCAPS-1D simulation," *Micromachines*, 12(12), 1508, 2021.

[12] T. AlZoubi, A. Moghrabi, M. Moustafa, and S. Yasin, "Efficiency boost of CZTS solar cells based on double-absorber architecture: Device modeling and analysis," *Solar Energy*, 225, 44-52, 2021.

[13] A. Houimi, S. Y. Gezgin, B. Mercimek, and H. Ş. Kılıç, "Numerical analysis of CZTS/n-Si solar cells using SCAPS-1D. A comparative study between experimental and calculated outputs," *Optical Materials*, 121, 111544, 2021.

[14] M. Sreejith, D. Deepu, C. S. Kartha, K. Rajeevkumar, and K. Vijayakumar, "Tuning the properties of sprayed CuZnS films for fabrication of solar cell," *Applied physics letters*, 105(20), 202107, 2014.

[15] Y. Khaaissa *et al.*, "Experimental and numerical simulation of deposition time effect on ZnS thin films for CZTS-based solar cells," *Optical and Quantum Electronics*, 53(9), 1-21, 2021.

[16] M. Burgelman, K. Decock, A. Niemegeers, J. Verschraegen, and S. Degrave, "SCAPS manual," ed: February, 2016.

[17] P. K. Kalita, B. Sarma, and H. Das, "Structural characterization of vacuum evaporated ZnSe thin films," *Bulletin of Materials Science*, 23(4), 313-317, 2000.

[18] S. Prabahar and M. Dhanam, "CdS thin films from two different chemical baths—structural and optical analysis," *Journal of Crystal Growth*, 285(1-2), 41-48, 2005.

[19] T. Raadik *et al.*, "Temperature-dependent photoreflectance study of Cu2SnS3 thin films produced by pulsed laser deposition," *Applied Physics Letters*, 110(26), 261105, 2017.

[20] P. Zhao and S. Cheng, "Influence of sulfurization temperature on photoelectric properties Cu2SnS3 thin films deposited by magnetron sputtering," *Advances in Materials Science and Engineering*, 2013, 2013.

[21] E. Hossain *et al.*, "Effects of sulfurization temperature on structural, morphological, and optoelectronic properties of CTS thin films solar cells," *Chalcogenide Letters*, 15(10), 499-507, 2018.

[22] D. Tiwari, T. K. Chaudhuri, T. Shripathi, U. Deshpande, and R. Rawat, "Non-toxic, earth-abundant 2% efficient Cu2SnS3 solar cell based on tetragonal films direct-coated from single metal-organic precursor solution," *Solar Energy Materials and Solar Cells*, 113, 165-170, 2013.

[23] A. D. Adewoyin, M. A. Olopade, O. O. Oyebola, and M. A. Chendo, "Development of CZTGS/CZTS tandem thin film solar cell using SCAPS-1D," *Optik*, 176, 132-142, 2019.

[24] B. Barman and P. Kalita, "Influence of back surface field layer on enhancing the efficiency of CIGS solar cell," *Solar Energy*, 216, 329-337, 2021.

[25] M. A. Shafi *et al.*, "Optimization of Electrodeposition Time on the Properties of Cu2ZnSnS4 Thin Films for Thin Film Solar Cell Applications," 2021.

[26] N. Khemiri, S. Chamekh, and M. Kanzari, "Properties of thermally evaporated CZTS thin films and numerical simulation of earth-abundant and non toxic CZTS/Zn (S, O) based solar cells," *Solar Energy*, 207, 496-502, 2020.

[27] L. Et-taya, T. Ouslimane, and A. Benami, "Numerical analysis of earth-abundant Cu2ZnSn (SxSe1-x) 4 solar cells based on Spectroscopic Ellipsometry results by using SCAPS-1D," *Solar Energy*, 201, 827-835, 2020.

[28] A. Srivastava, P. Dua, T. Lenka, and S. Tripathy, "Numerical simulations on CZTS/CZTSe based solar cell with ZnSe as an alternative buffer layer using SCAPS-1D," *Materials Today: Proceedings of*, 43, 3735-3739, 2021.

[29] S. Meher, L. Balakrishnan, and Z. Alex, "Analysis of Cu2ZnSnS4/CdS based photovoltaic cell: a numerical simulation approach," *Superlattices and Microstructures*, 100, 703-722, 2016.

[30] A. Mohandes, M. Moradi, and H. Nadgaran, "Numerical simulation of inorganic Cs2AgBiBr6 as a lead-free perovskite using device simulation SCAPS-1D," *Optical and Quantum Electronics*, 53(6), 1-22, 2021.

[31] V. Raj, F. Rougieux, L. Fu, H. H. Tan, and C. Jagadish, "Design of Ultrathin InP Solar Cell Using Carrier Selective Contacts," *IEEE Journal of Photovoltaics*, 10(6), 1657-1666, 2020.

[32] H. Fu and Y. Zhao, "Efficiency droop in GaInN/GaN LEDs," in *Nitride Semiconductor Light-Emitting Diodes (LEDs)*: Elsevier, 299-325, 2018.

[33] F. Staub, U. Rau, and T. Kirchartz, "Statistics of the Auger recombination of electrons and holes via defect levels in the band gap—application to lead-halide perovskites," *ACS Omega*, 3(7), 8009-8016, 2018.

[34] P. Roy, S. Tiwari, and A. Khare, "An investigation on the influence of temperature variation on the performance of tin (Sn) based perovskite solar cells using various transport layers and absorber layers," *Results in Optics*, 4, 100083, 2021.

[35] M. Abderrezek, M. Fathi, and F. Djahli, "Comparative study of temperature effect on thin film solar cells," 2018.

[36] H. Zhang, S. Cheng, J. Yu, H. Zhou, and H. Jia, "Prospects of Zn (O, S) as an alternative buffer layer for Cu2ZnSnS4 thin-film solar cells from numerical simulation," *Micro & Nano Letters*, 11(7), 386-390, 2016.

[37] L. I. Nykyruy et al. "Evaluation of CdS/CdTe thin film solar cells: SCAPS thickness simulation and analysis of optical properties." *Optical Materials*, 92, 319-329, 2019.

[38] A. D. Adewoyin, et al. "Development of CZTGS/CZTS tandem thin film solar cell using SCAPS-1D." *Optik*, 176, 132-142, 2019.

[39] Zyoud, Samer H., et al. "Numerical modeling of high conversion efficiency FTO/ZnO/CdS/CZTS/MO thin film-based solar cells: Using SCAPS-1D software." *Crystals*, 11(12), 1468, 2021.